Stability of Aqueous Silica Nanoparticle Dispersions under Subsurface Conditions

Cigdem O. Metin [*], Larry W. Lake [*], Caetano R. Miranda [**] and Quoc P. Nguyen [*]

[*] Petroleum and Geosystems Engineering Department, The University of Texas at Austin, 1 University Station , C0300 Austin, TX 78712-1061, USA,
cigdem@mail.utexas.edu, larry_lake@mail.utexas.edu, quoc_p_nguyen@mail.utexas.edu
[**] Universidade Federal do ABC, Rua Santa Adélia, 166, CEP 09210-170, SP, Brazil,
caetano.miranda@ufabc.edu.br

ABSTRACT

We present quantification methods for nanoparticle stability analysis using non-intrusive analytical techniques to study the stability of silica nanoparticle dispersions and the effects of pH, temperature and electrolytes that would be encountered in oil field brines in a reservoir. Spectral analysis of the Si-O bond at wavenumber of 1110 cm^{-1} with the attenuated total reflectance, Fourier transform infrared (ATR-FTIR) indicates a structural change on the surface of silica particles as the dispersion pH changes. We define a critical salt concentration (CSC) for, NaCl, $CaCl_2$, $BaCl_2$ and $MgCl_2$, above which the silica dispersion becomes unstable. Divalent cations Mg^{2+}, Ca^{2+} and Ba^{2+} are more effective in destabilizing silica nanoparticle dispersion than the monovalent cation Na^+. The CSC for Na^+ is about 100 times more than for Ca^{2+}, Ba^{2+} and Mg^{2+}. Among the divalent cations studied, Mg^{2+} is the most effective in destabilizing the silica particles. The CSC is independent of silica concentration, and lowers at high temperature.

Keywords: silica nanoparticles, aqueous stability, temperature, electrolytes, aggregation

1 INTRODUCTION

In the recent years, nanotechnology has drawn the attention of many researchers to develop innovative solutions to satisfy the growing demand in hydrocarbons. The potential application of nanoparticle dispersions has significantly advanced into the upstream oil and gas industry, from drilling, formation characterization, to improved hydrocarbon and geothermal heat recovery [1]. The success of these potential applications depends on the ability to control the stability [2] of nanoparticle dispersions.

Silica dispersions have been of interest in colloidal science because of their many applications and because their anomalous behavior [3] of particle aggregation may not be predicted by Derjaguin-Landau-Verwey-Overbeek (DLVO) theory [4, 5]. The increasing rate of aggregation of silica nanoparticles with concentration of electrolytes is known but not well understood [6].

In this paper, we present a systematic study of the stability of silica nanoparticle dispersions. The effect of pH on the colloidal stability of silica is determined by different analytical methods. We identify a critical salt concentration (CSC) for different monovalent (NaCl) and divalent cations ($CaCl_2$, $MgCl_2$ and $BaCl_2$) above which silica nanoparticle dispersion becomes unstable. Development of quantitative methods for determining the CSC is discussed. The effect of temperature on the CSC is also investigated. Detailed study on the phase behavior of silica dispersions is also presented.

2 MATERIAL AND METHODS

The material understudy is an aqueous dispersion of silica particles that have a mean diameter of 25nm and an unmodified (bare) surface. The shape and size of silica particles were examined by a Hitachi-S5500 scanning transmission electron microscope (STEM). The result from dynamic light scattering (DLS) measurements also shows a mean diameter of 25nm with a polydispersity index of 0.077 indicating a narrow size distribution.

A stock solution containing 41.13% by weight silica nanoparticles was diluted with deionized water up to a desired silica concentration. NaCl, $MgCl_2$, $BaCl_2$ and $CaCl_2$ were the inorganic salts that we used in the experiments. All chemicals were of analytical grade quality.

A spectrum 100 FTIR spectrometer made by Perkin Elmer was used to identify chemical functional groups present in the silica nanoparticles and their dispersions. We also used a Cary 50 ultraviolet-visible spectrophotometer (UV-Vis) of to analyze optical absorbance of silica dispersions. The absorbance-time relationship provided a means to study the aggregation of silica dispersions. We used a zeta potential analyzer (Zeta Plus) with a dynamic light scattering option from Brookhaven Instruments Corporation to determine the zeta potential and effective particle diameter of silica nanoparticle dispersions.

3 RESULTS AND DISCUSSION

3.1 The effect of pH on aqueous stability of silica nanoparticle dispersion

Figure 1 shows the respective ATR-FTIR transmittance spectra of deionized water, a dry silica sample, and a silica dispersion sample with a pH of 9.65. Deionized water

shows a broad peak at 3330 cm^{-1} and a sharp peak at 1629 cm^{-1} because of the stretching and bending vibrations of the O-H bonds in the water molecules. Comparing the spectra of deionized water and the silica dispersion reveals the presence of silica nanoparticles by a characteristic Si-O peak at 1100 cm-1. The deionized water curve coincided with the silica dispersion at the peaks corresponding to vibrations of O-H bonds. In the spectrum of silica powder, two peaks corresponding to Si-O bond vibration occur at 793.4 and 1055.3 cm^{-1}. Morrow and Molapo [7] also observed similar peaks at 1100 and 800 cm^{-1} for a silica thin film. A small and broad peak at 3300 cm^{-1} and a small peak at 1650 cm^{-1} in the spectrum of the silica powder indicate the presence of adsorbed water that remains after drying. The transmittance corresponding to the Si-O peak at 1100 cm^{-1} in the silica dispersion is large compared to silica powder because of the small concentration of silica nanoparticles (1 wt%) in the dispersion. Moreover, the Si-O peak at 793.4 cm^{-1} observed with powder silica particles is suppressed by water in silica dispersions (Fig. 1). Therefore, only the Si-O peak at 1100 cm^{-1} is used to evaluate the effect of pH on the aqueous stability of a silica nanoparticle dispersion.

We measured the infrared light (IR) transmittance of two respective series of 0.5 and 1 wt% silica particle dispersions, whose pH varied over a wide range from 2.5 to 10. All of these samples exhibit a stable clear phase, indicating an indiscernible effect of pH on the stability of silica nanoparticle dispersion. However, a plot of Si-O peak area, which is the area under the peak at 1100 cm^{-1}, versus pH, suggests a significant variation of silica nanoparticle surface structure with pH. The peak area first decreases sharply as pH increases, and then levels off at around a pH=7, regardless of particle concentration. A small increase in the peak area at a given pH is because of an increase in particle concentration.

The surface charge of metal-oxide particles in water may vary from positive to negative as pH increases because of surface deprotonation [8]. The isoelectric point, defined as the pH at which the surface is neutrally charged, measures the structure of a charged surface. The measured zeta potential representing the surface potential [8] of the silica nanoparticles as a function of pH is in Fig. 2. It fluctuates around a constant value of -45mV as pH decreases from 10 to 6, but sharply increases with further decrease in pH. This trend is observed for both 0.5 and 1 wt% particle concentrations, which is consistent with the relationship between IR transmittance and pH. Furthermore, extrapolating the potential curve to the smaller pH range in Fig. 2 suggests that the silica surface approaches the isoelectric point at a pH around 3.44.

The pH-induced aggregation of silica particles is not seen by visual observation because of the possible nanometer-sizes of aggregates. Another way to identify the presence of nanoparticle aggregation is through the ultraviolet-visible spectroscopy (UV-Vis) and dynamic light scattering (DLS). The absorbance does not significantly change with pH. This evidences the absence of particle aggregation, which is confirmed by the results from the DLS measurements. The effective particle diameter increases by a factor of 1.36 as pH decreases from 10 to 2. Therefore, particle aggregation is not responsible for the observed slight change of the effective particle diameter with pH despite of the significant pH-induced reduction of particle surface charge (see Fig. 2).

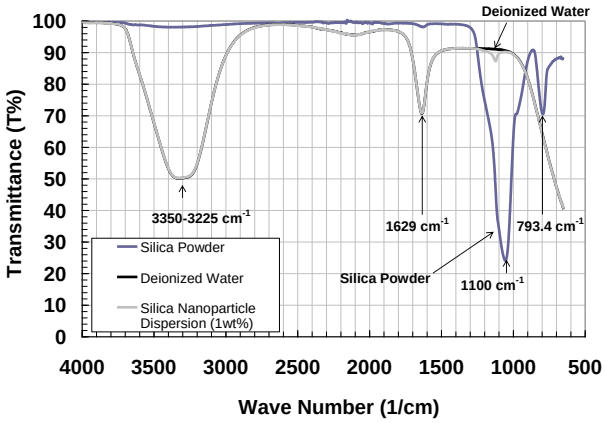

Figure 1: ATR-FTIR transmission spectrum of dried silica powder, 25nm silica particle dispersion, and deionized water.

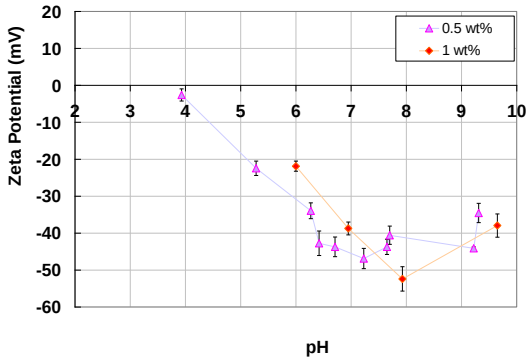

Figure 2: Zeta potential of silica particle dispersions as a function of solution pH.

3.2 Phase behavior of silica nanoparticle dispersions in presence of electrolytes

Electrolytes could also destabilize particle dispersions by compressing the electrical double layer. As the electrolyte concentration increases, the energy barrier is lowered to an extent that kinetic energy of particles dictates the kinetics of particle aggregation [4, 5]. Figure 3 shows the phase behavior of silica dispersions that are different in NaCl and particle concentrations. For small particle concentration (e.g. 0.5 wt% particle in Fig. 3), the addition of NaCl up to around 1.5 wt% does not destabilize the aqueous dispersion of silica nanoparticles. However, a further increase in NaCl concentration leads to a phase transition. This phase behavior suggests that 1.5 wt% NaCl

represents a critical salt concentration (CSC) above which particle aggregation and sedimentation visually occurs. When the NaCl concentration is increased above its CSC, three distinct subsequent stages of particle aggregation could be observed: (1) an early-time stage characterized with a single clear phase (e.g. vials shown in Fig. 3 with 0.5 wt% particle concentration and 3 wt% NaCl at 1 hour), (2) a precipitation stage with a single turbid phase (e.g. same vials at 10 days later), and (3) a sedimentation stage with two separate phases (e.g. the same vials after 41 days). The subsequent occurrence of the precipitation and sedimentation stages is accelerated by either increasing NaCl or particle concentration. For example, Fig. 3 shows that for 2 wt% NaCl concentration the particle dispersion with 2 wt% particle concentration approaches the end of the precipitation stage after 10 days while the dispersion with 0.5 wt% particle concentration is still in the early-time stage. However, these two factors were found not to significantly influence the CSC for NaCl.

Figure 4 shows that the absorbance profile for 0.5 wt% particle concentration at 400nm wavelength is characterized by a transition from a uniform to a sharp increase as NaCl increases above a critical value. This critical value does change with time (i.e. from 2 wt% at 1 hour to 1 wt% after 43 days) and eventually reaches a constant value of 1 wt%, which defines the equilibrium CSC for NaCl. The variations of effective particle diameter in time and with NaCl concentration are also presented in Fig. 4. The effective particle diameter profiles are very close to the UV-Vis light absorbance profiles. Both techniques give almost the same CSC.

3.3 Effect of divalent cations on critical salt concentration (CSC)

For both Mg^{2+} and Ca^{2+}, an increase in concentration above a critical value gives rise to particle aggregation, in consistence with the phase behavior for NaCl. A silica particle dispersion exhibits an equilibrium clear phase for divalent cation concentration lower than 0.02 wt% (Fig. 5), which is hundred times lower than that for the monovalent cation (CSC for NaCl is 1 wt%). For a divalent cation concentration above 0.04 wt%, the particle aggregation is so effective that the early-time stage is almost absent; sedimentation begins only after 1 day. Among these cations, Mg^{2+} exhibits the most capability of particle dispersion destabilization. The CSCs, determined at a point of sharp change in UV-Vis absorbance profiles, are 0.0125 wt% for $MgCl_2$ and 0.025 wt% for both $CaCl_2$ and $BaCl_2$. These values are confirmed by the measured effective particle diameter as a function of salt concentration.

The significant difference in CSC between the monovalent and divalent cations could be further explained by the DLVO theory [4, 5]. A secondary minimum in energy occurs at NaCl concentrations greater than 1 wt% in Fig. 6. The area under the DLVO curve as a function of electrolyte concentration shows the relationship between electrolyte concentration and the amount of energy required to bring two nanoparticles from infinity to a critical distance that is shorter than that at which particle aggregation is highly promoted. This integration term decreases first sharply then much more gradually as electrolyte concentration increases. This gradually decreasing slope, in the region between 0.5 and 1.5 wt% NaCl, is the region where the transition of a stable dispersion into an unstable state occurs. The range of electrolyte concentration for this transition region is significantly reduced as the cation's valence increases and is consistent with the measured CSCs for Na^{+}, Ca^{2+}, and Mg^{2+}.

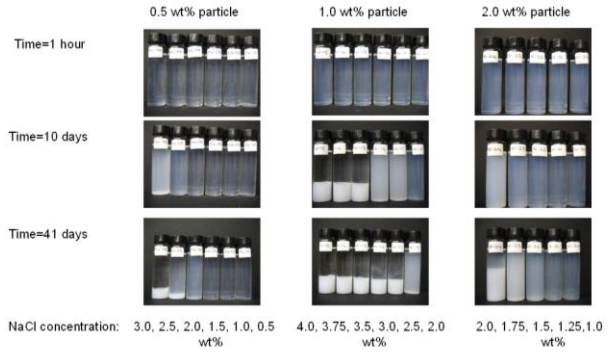

Figure 3: Phase behavior of silica nanoparticle dispersions at various NaCl and nanoparticle concentrations.

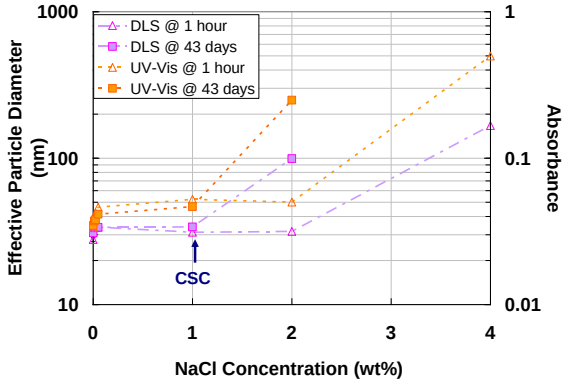

Figure 4: DLS and UV-Vis absorption at 400nm wave length for 0.5 wt% silica dispersions

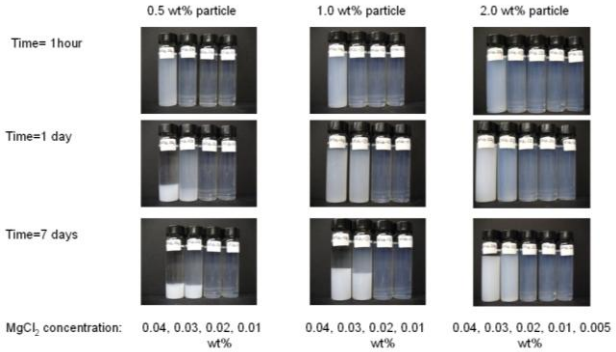

Figure 5: Phase behavior of silica nanoparticle dispersions at various $MgCl_2$ and nanoparticle concentrations.

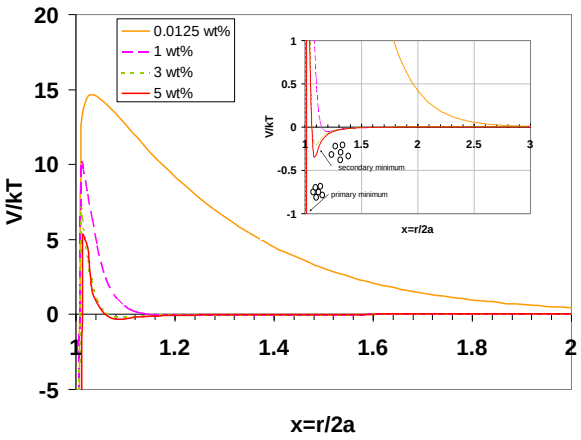

Figure 6: Two-particle interaction potential as a function of dimensionless separation distance according to DLVO theory for NaCl concentrations

3.4 Effect of Temperature on critical salt concentration

To investigate the effect of temperature on the CSC, we used DLS to measure particle size on a series of 1 wt% silica dispersions with different salt types (NaCl, $CaCl_2$ and $MgCl_2$) and concentrations at 25 and 70°C. The results, shown in Fig. 6, indicate that the CSC is significantly reduced as temperature increases. This observation could be explained by the fact that an increase in temperature causes the collision frequency of the colloidal particles to increase as well as their kinetic energy. This promotes successful particle collision and aggregation.

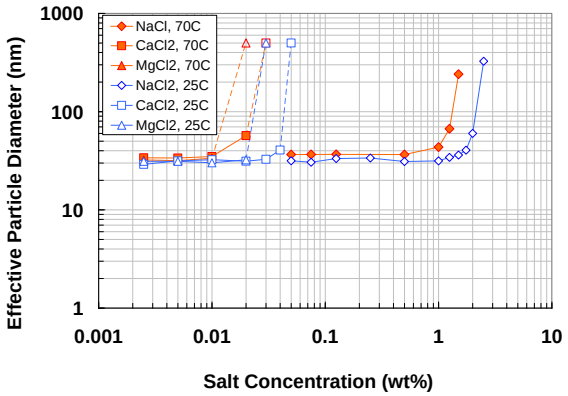

Figure 6: DLS measurements of 1 wt% silica dispersion in the presence of different salts (NaCl, $CaCl_2$ and $MgCl_2$) at 25°C and 70°C.

4 CONCLUSIONS

Spectral analysis of the Si-O bond at 1110 cm^{-1} with the ATR-FTIR indicates a structural change on the surface of silica particles because of the change in the pH of the solution, which agrees with zeta potential results. Changing the pH does not affect the aggregation in the absence of electrolyte for the range of pH studied. However, the addition of different types of salts (NaCl, $CaCl_2$, $MgCl_2$ and $BaCl_2$) causes aggregation of the silica nanoparticles.

We observed a critical salt concentration (CSC) for a given electrolyte below which the silica nanoparticles are well dispersed in an aqueous phase and above which flocculation of silica nanoparticles occur and the aggregates settle by gravity. The CSC depends on electrolyte type, but is not influenced by silica nanoparticle concentration.

Divalent cations Mg^{2+}, Ca^{2+} and Ba^{2+} were more effective in destabilizing (i.e. causing aggregation) the nanoparticle dispersion than the monovalent cation Na^{+}. The CSC for Na^{+} (1.5 wt% NaCl) is about 100 times larger than that of divalent cations (0.02 wt% for Mg^{2+} and 0.03 wt% for Ca^{2+} and Ba^{2+}). Among these divalent cations, Mg^{2+} is the most effective in aggregating the silica particles. The DLVO theory explains the presence of CSC for the electrolytes studied.

An increase in temperature from 25°C to 70°C increases the aggregation rate, and hence lowers the CSC. The CSC reduction is 67%, 50%, and 33% for Na^{+}, Mg^{2+}, and Ca^{2+}, respectively.

5 ACKNOWLEDGMENT

This work is supported by the Advanced Energy Consortium (AEC), through the contract BEG08-020. We would thank 3M company, particularly Dr. Jimmie R. Baran for providing the nanoparticles. We would also like to acknowledge great help from Dr. Sujeewa Palayangoda and Ms. Wenjun Liu.

REFERENCES

[1] S. Mokhatab, M.A. Fresky, M.R. Islam, J. Pet. Technol. 58 (2006) 4.
[2] E. Kissa, Dispersions: Characterizations Testing, and Measurement, Marcel Dekker,New York, 1999.
[3] T.W. Healy, in: H.E. Bergna, W.O. Roberts (Eds.), Colloidal Silica: Fundamentals and Applications, CRC Press, Boca Raton, 2006, p.247.
[4] B.V. Derjaguin, L. Landau, Acta Physicochim., USSR, 14 (1941) 633.
[5] E.J.W. Verwey, J.Th.G. Overbeek, Theory of Stability of Lyophobic Colloids, Elsevier, Amsterdam, 1948.
[6] W.O. Roberts, in: H.E. Bergna, W.O. Roberts (Eds.), Colloidal Silica: Fundamentals and Applications, CRC Press, Boca Raton, 2006, p.131.
[7] B.A. Morrow, D.T. Molapo, in: H.E. Bergna, W.O. Roberts (Eds.), Colloidal Silica: Fundamentals and Applications, CRC Press, Boca Raton, 2006, p.287.
[8] R.J. Hunter, Foundations of Colloid Science, Oxford, New York, 2001.
[9] J.A. Kitchener, Faraday Disc. 52 (1971) 379.
[10] R.K. Iler, The Chemistry of Silica, Wiley & Sons, New York, 1979, p.367.
[11] J. Israelachivili, H. Wennerstrom, Nature 379 (1996) 219.